# Dipole Assisted Photogated Switch in Spiropyran Grafted Polyaniline Nanowires

Yosef Bardavid,[†] Ilya Goykhman,[‡] Daijiro Nozaki,[§] Gianaurelio Cuniberti,[§] and Shlomo Yitzchaik*,[†]

[†]Institute of Chemistry, [‡]Department of Applied Physics, The Center for Nanoscience and Nanotechnology, The Hebrew University of Jerusalem, Jerusalem 91904, Israel

[§]Institute for Materials Science and Max Bergmann Center of Biomaterials, Dresden University of Technology, Dresden 01062, Germany

ABSTRACT: In this work we show dipole-assisted photogated switching by covalent grafting of photoactive molecules to conducting polymers. Photochromic spiropyran molecules were covalently attached to polyaniline (PANI) nanowires via N-alkylation reaction to the quinoic part of PANI. Upon irradiation with ultraviolet light spiropyran transformed to a large dipole containing molecule, merocyanine form. We show that this transformation leads to a substantial (ca. 2 orders of magnitude) increase in conductance of the photochromic PANI nanowires, which were evident by an increase in field-effect mobility and calculated band gap narrowing of the system. Finally, this transformation was found to be fully reversible with no significant photofatigue.
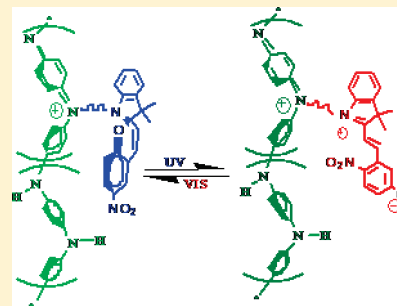
INTRODUCTION

Creating photoresponsive molecularly decorated nanomaterials is an attractive assembly route toward new functional architectures in molecular electronic and optoelectronic devices.[1,2] Converting optical radiation to electrical signals[3–6] or magnetic signals[7–12] with nanoscale precision is an ongoing challenging task in contemporary research. Recently we witnessed the realization of nanoscale photoactive devices decorated with photochromic molecules such as photosensitive field effect transistors (FET) based on carbon nanotubes (CNT).[13–15] It has been shown that electrical properties of CNTs can be affected by irradiation and the corresponding reversible modulation of conductance can be obtained employing structural changes in the photochromic molecules.

Along with investigations into conducting polymers, it has been reported that introduction of photoresponsive materials into the side- or main-chain of conducting polymers can also preserve their photoisomerization.[16–19] Photochromic characteristics of conjugated polymers such as polyacetylene, polyaniline, and poly(p-phenylenevinylene) derivatives containing photochromic azobenzene moieties in the side-chain have been studied. Still, these works did not examine the effect of illumination on the conductivity of these systems.

Polyaniline (PANI) is one of the most investigated conducting polymers due to its unique features such as versatile redox properties, environmental stability, and reversible doping.[20,21] PANI nanowires and nanotubes are attracting interest in the nanosciences because of their unique electrical, mechanical, and optical properties, which are placing them at the forefront of promising materials for versatile electrical and optical applications such as molecular sensors and electronic displays.[22,23] At the same time, in the class of photoactive materials, spiropyran (SP) molecules are among the most studied photochromic molecules. SPs can undergo photoinduced

ring-opening under UV irradiation by homolytic cleavage of the C–O bond (spiro carbon to furan oxygen), yielding the merocyanine (MC) form that in turn contains a large molecular dipole.[24,25] SP molecule was suggested[26] as a candidate for controlling the electrical properties of PANI based on proton doping and dedoping mechanism in blended thin films of PANI and SP. In this blend, MC acts as a hydrogen acceptor from PANI and therefore decreases the conductivity of the mixed layer by PANI dedoping. The reversible process is promoted by irradiation with visible light where SP acts as a hydrogen donor to PANI resulting in restoring the initial conductance. To that end, in the blended form, the system suffers from a limited change in the conductivity (about two times) and from inherent instability most probably owing to the phase separated nature of such a blend.

Herein, we demonstrate a stable, dipole-assisted photogated switch in spiropyran covalently linked polyaniline nanowires. Our experimental results and theoretical calculations indicate that irradiation of the system based on covalent bonding of SP molecules as side group to PANI nanowires can yield reversible and substantial changes (about 2 orders of magnitude) in the conductivity of PANI, which we refer to molecular dipole changes of photochromic molecules. We also demonstrate that the significant enhancement of conductivity following UV irradiation is related to increase in holes mobility.
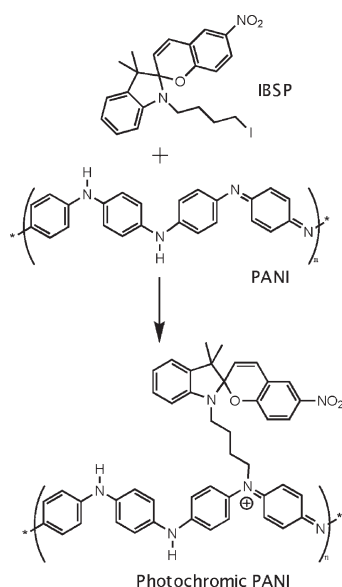
EXPERIMENTAL DETAILS

Synthesis of PANI nanowires were carried in the following way: 28 mM aniline was dissolved in CH_2Cl_2 and mixed with the

Scheme 1. Synthetic Route Towards Grafting Photochromic Spiropyran on Polyaniline (PANI) Nanowires

7 mM of ammonium peroxydisulfate in 1 M of HCl in water. After several minutes, green polyaniline migrates from the organic phase to the aqueous phase; after 3 h of reaction, nanowires are purified by centrifugation (3×) at 3000 rpm for 0.5 h. Colloids of PANI nanowires were prepared in 1 M HCl, and the solution was used for immobilizing the PANI nanowires between two gold electrodes. Prior to the modification with spiropyran, the PANI nanowires network modified electrodes were immersed into the NH₄OH solution for 10 min for the formation of the emeraldine base form of PANI. 1-(4-Iodobutyl)-3,3-dimethylindoline-6-nitrobenzospiropyran (IBSP) was prepared according to the literature[27] and its structure is shown in Scheme 1. The modification of the PANI nanowires with spiropyran, were performed by incubating the electrodes with 1 mM solution of IBSP dissolved in DMF for 2 h, the sample is then washed and dried with N_2. Subsequent to the grafting reaction the sample is heated to 60 °C for 20 min to convert any open structure of merocyanine to the close form of SP.

To clarify the formation of photochromic nanowires, X-ray photoelectron spectroscopy (XPS) was applied and measurements were performed using a Kratos Axis Ultra instrument. The UHV chamber had a base pressure of 10^{-9} Torr, and the samples were transported to the instrument under a nitrogen atmosphere. All samples were entered into the UHV chamber at the same time, and were measured sequentially. The 225 W monochromated Al Kα X-ray beam was used ($E = 1486.7$ eV) for the analysis. The measurements were taken under a Pass Energy of 20 eV and an energy step of 0.1 eV. Spectra were acquired twice, once fast (dwell time of 1 s) to check that the sample is not damaged under the X-ray beam and once slow (dwell time of 1 s, 15 sweeps) to get good signal-to-noise ratio. All energies were calibrated against the C 1s peak (284.9 eV). FTIR spectra were recorded in the CaF₂ cell (0.01 mm) in a Bruker IFS-113v spectrometer. The polymer film for FTIR measurement was prepared by heating the powder at 180 °C between CaF₂ plates. High resolution scanning electron microscope (HRSEM) images were carried out on a FEI Sirion system for the PANI-NW deposited on Si ⟨100⟩ substrates.
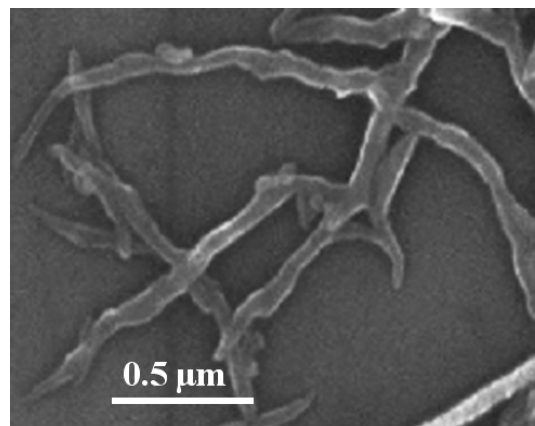

Figure 1. HRSEM micrograph of PANI nanowires. The obtained dimensions are 40–60 nm width and 1–1.5 μm length.
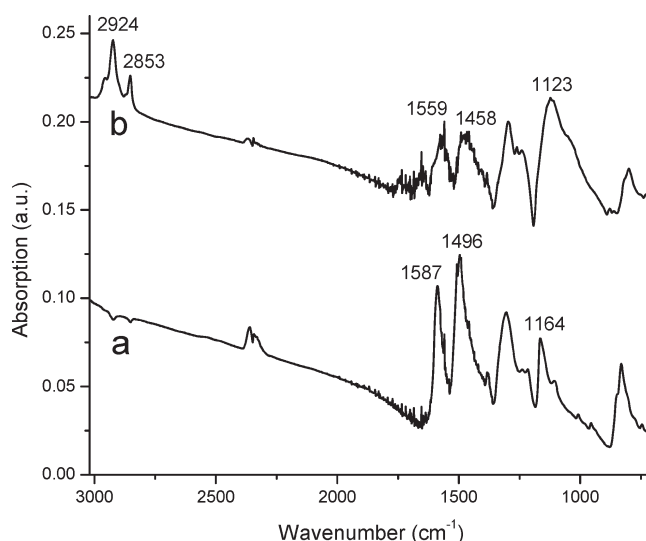

Figure 2. FTIR spectra of photochromic PANI-NW: (a) PANI before and (b) after SP grafting (PANI-SP).

For electrical characterization of the photochromic nanowires' layer we have employed a bottom-gate configuration of the field effect transistor (FET). First, a highly doped silicon substrate was thermally oxidized (200 nm) to realize a gate insulator. Next, an aluminum pad was evaporated to the back side of the wafer to make a gate contact. The source and drain electrodes were patterned by e-beam lithography, followed by gold metallization and lift-off processes to obtain a final width and length of single transistor of 200 and 4 μm, respectively (see also, Figure 7a).

■ RESULTS AND DISCUSSION

Following the synthesis and chemical modification of PANI nanowires, we took high resolution scanning electron microscope (HRSEM) micrograph of the system as it is presented in Figure 1. According to HRSEM image the obtained typical dimensions of nanowires bundle are 40–60 nm width and 1–1.5 μm length.

In the first part of this study we confirmed the grafting of SP groups on PANI nanowires (Scheme 1) by Fourier transform infrared spectroscopy (FTIR) and X-ray photoelectron spectroscopy (XPS). FTIR analysis of PANI nanowires before and after the grafting of SP groups is shown in Figure 2. The presence of
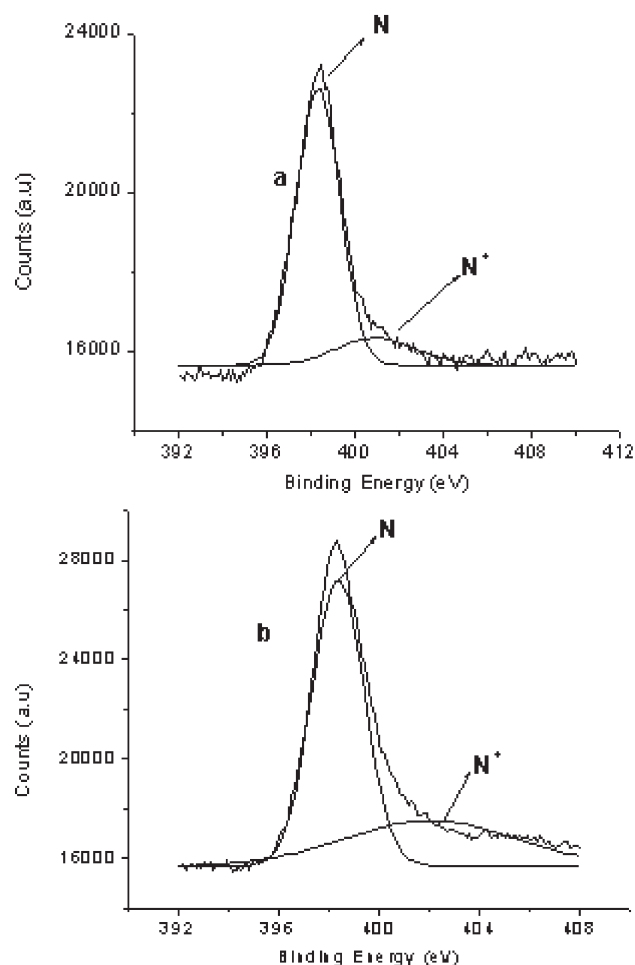
Figure 3. XPS spectra of photochromic PANI-NW: (a) PANI before and (b) after SP grafting (PANI-SP).

Figure 4. Current−voltage characteristics of photochromic PANI-NW: (a) before and (b) after SP grafting (PANI-SP).

Figure 5. Current−voltage characteristics of photochromic PANI-NW: (a) before irradiation (PANI-SP) and (b) after irradiation (PANI-MC) with UV light.

the aliphatic spacer connecting SP to PANI is evident from the methylene symmetric and asymmetric stretching at 2853 and 2924 cm^{-1}, respectively. In the aromatic region of the vibrational spectra PANI and SP overlap, however, the characteristic peaks at 1587 and 1496 cm^{-1} for the PANI have been associated with the aromatic ring stretching of the quinoid and benzoid ring, respectively. Subsequent to the reaction with IBSP, an increase in the intensity and the broadening of the imine peak at 1123 cm^{-1} is observed, which implies some degree of electron delocalization and an increase in the electrical conductivity.[28−30] Additionally, the decrease in the intensity and red shifting of IR peaks from 1587 and 1496 cm^{-1} to 1559 and 1458 cm^{-1} are the characteristics of the emeraldine salt,[31−34] which indicates the imine group's quaternization and increase in electrical conduction due to such doping.

In parallel to FTIR analysis, PANI-nanowire quaternization is also verified by XPS measurements (see Figure 3). The peak obtained around 399 eV corresponds to the tertiary nitrogen (N) atom and the peak around 401 eV corresponds to the quaternary nitrogen (N$^+$) atom.[35,36] The ratio, between these atoms N$^+$/N calculated from the area is 0.05, increases to 0.30 following SP grafting on the PANI nanowires. Taking into account the molecular weight ratio of the repeating units before and after the reaction, we evaluated that about 20% of the repeating units of doped (quarternized) PANI nanowires are grafted by SP molecules.
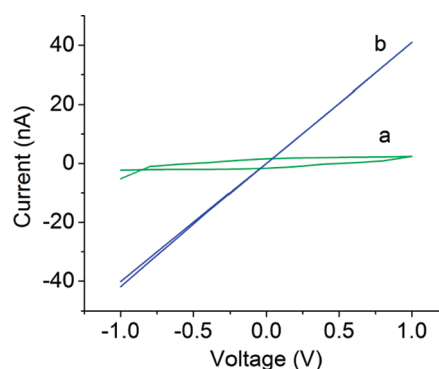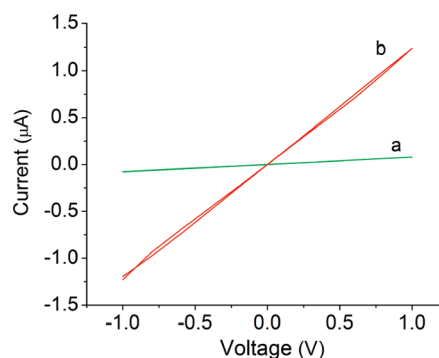
The electrical characteristics of PANI nanowires were noticeably changed following the grafting of SP photochroms on these nanowires. Figure 4 shows the current−voltage (I−V) characteristics of nanowires before and after the reaction with spiropyran. SP-grafted nanowires exhibited a 20-fold increase in the current (from 2 to 40 nA) compared to SP-free PANI nanowires and linear current−voltage relation, over −1 V to +1 V potential window. The increase in conductivity following the N-alkylation reaction is attributed to the covalent bonding of SP molecules to PANI-nanowires through imine nitrogen's quaternization and PANI doping, which is similar to the conventional chemical-doping routes in the literature.[35,36] This action increases the concentration of the charge carriers in line with the observed FTIR spectral broadening of the imine peak.

Next to confirming the grafting of SP groups on PANI nanostructure and electrical properties of the decorated nanowires, we investigated the photoswitching and electrical transport properties of this system. The current−voltage (I−V) characteristics of the system are shown in Figure 5. Experimental results show a large changes in the conductance of the system upon the irradiation with UV light (ca. λ = 365 nm). At this wavelength SP molecules are photoswitched (Scheme 2) to their charge separated merocyanine form characterized by a large (about 50 D) molecular dipole moment. It can be clearly seen that upon irradiation and the formation of molecular dipoles the current increases drastically (from 40 nA to 1.2 μA) for bias voltage of 1 V. The reversibility of the process was confirmed by heating or

3125

dx.doi.org/10.1021/jp110665j |*J. Phys. Chem. C* 2011, 115, 3123–3128

by exposure of the sample to visible light (ca. $\lambda \geq 500$ nm). After the heating or visible light exposure, the conductivity of the PANI-MC decreases back nearly to its original value of PANI-SP. Figure 6 shows several cycles alternating in the grafted PANI nanowires between the spiropyran (SP) and merocyanine (MC) forms.

The reversible switching between the high and the low conductance states in modified PANI nanowires suggests that change in the transport properties is associated with the photochromism of grafted spiropyran molecules. To verify the molecular photoisomerization effect on the free carriers' mobility, we have

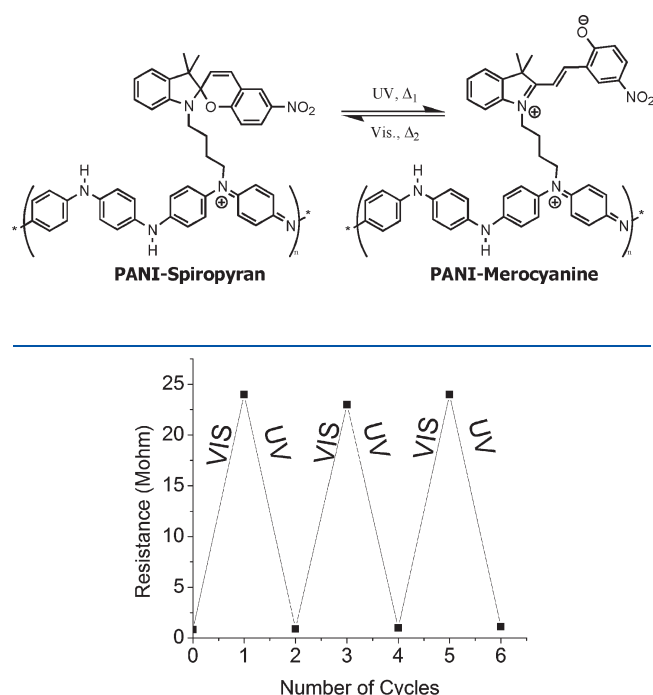**Scheme 2. Photochromism of Polyaniline (PANI) Nanowires**

performed field effect experiments before and after UV irradiation using photochromic PANI layer as the organic semiconductor layer and back-gated microelectronic configuration (see also, Figure 7a). On the basis of standard transfer characteristics of the organic field effect transistor (OFET) device, we calculated the transconductance of transistor (g_m) and found the mobility variation of charge carriers in the polymer layer due to irradiation. Figure 7b shows the transfer curves of the fabricated device with PANI-SP and PANI-MC organic layers. In linear operation regime, the transconductance of the FET structure is given by

$$g_m = \left. \frac{\partial I_{DS}}{\partial V_{DS}} \right|_{V_{DS}} = \frac{W}{L} i \times C_{ox} \times V_{DS} \qquad \text{(Eq. 1)}$$

where g_m is the transconductance, W and L are the channel width and length, respectively, μ is the effective mobility, and C_{ox} is the
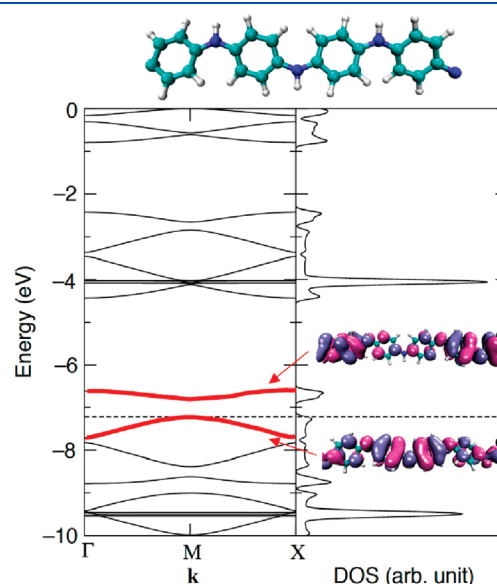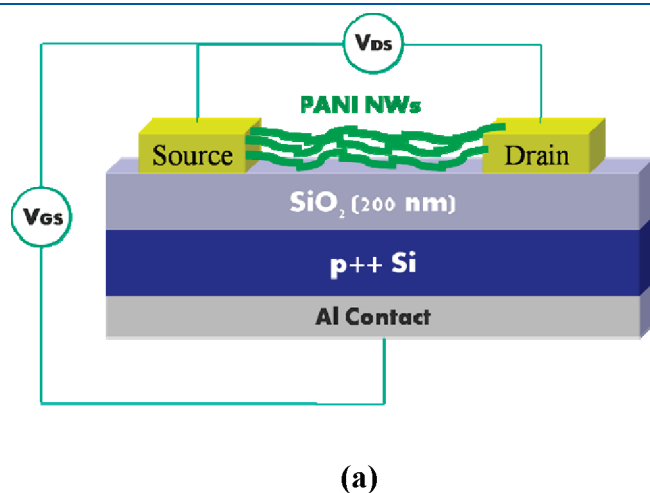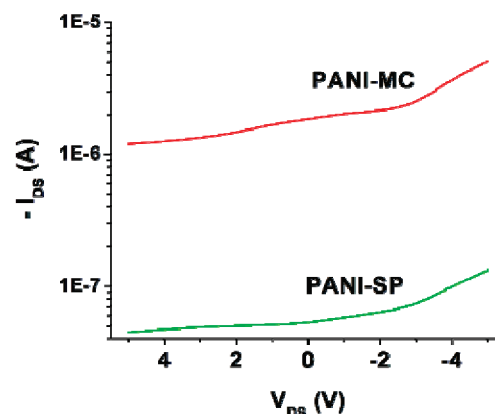

Figure 8. Band structures and DOS of PANI: The energy bands where the electronic orbitals delocalize over the main chains are shown in red. The Fermi energy is shown in the dotted line.

Figure 6. Light-induced electrical resistance changes in photochromic-PANI nanowires.

(a)

(b)

Figure 7. Field-effect measurement: (a) Schematic configuration of experimental setup; (b) Transfer characteristics of the OFET device at $V_{DS} = -1$ V for photochromic PANI-SP system (before UV irradiation) and PANI-MC system (after UV irradiation).
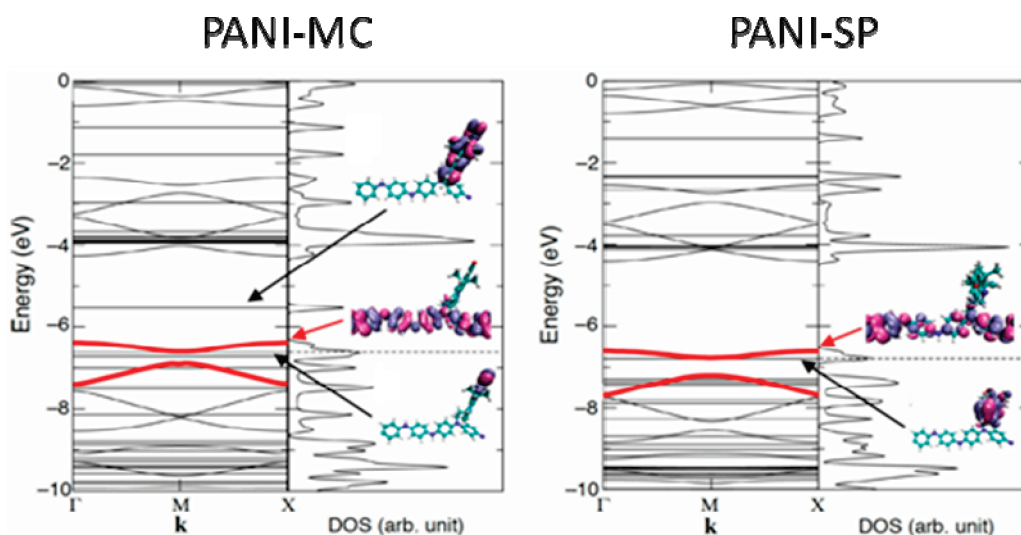
Figure 9. Band structures and DOS of PANI-MC and PANI-SP. The Fermi energy is shown in the dotted line. The energy bands where the electronic orbitals delocalize over the main chains are shown in red. The flat bands have a localized orbital on the side chains. These bands do not contribute to the charge transport.

capacitance per unit area of the insulating layer. For $V_{DS} = -1$ V, the hole mobility obtained from experimental results is 3.6×10^{-2} cm^2/(V s) for PANI-SP and $1.54 \times$ cm^2/(V s) for PANI-MC.

The relation between molecular dipole change and its influence on the conductance has been shown to affect transport properties of semiconductors and derived structures.[37,38] In particular, it was shown that transport properties of silicon devices that were grafted with spiropyran groups can be tuned reversibly by irradiation.[39] Merocyanine, as opposed to the spiropyran molecule, is highly polar and a polarizable molecule possessing a large (ground state) molecular dipole, about 50 D, may yield a significant change in the local electrostatic environment around the nanowires, such as scattering and localization of charge carriers, which are yielding the changes in the nanowire's conductance. Additionally, formation of merocyanine aggregates in polymers containing SP as side groups upon UV irradiation is well established.[25,40] This kind of physical cross-linking between the PANI nanowires may yield, in addition, enhancement of electrons percolation between neighboring nanowires. Upon closure of merocyanine to spiropyran in the reverse cycle, these effects disappear and conductivity decreases to its original value. Therefore, we relate the observed increase in hole mobility to the presence of molecular dipoles in the case of an irradiated system that have a vectorial component to increase the hopping probability from one conducting segment to the other.

To further investigate the photoinduced switching mechanism in spiropyran-attached PANI, we performed band calculations and compared the band structures between opened form (PANI-MC) and closed form (PANI-SP). At first, as a reference system, we investigated the band structure of spiropyran-free PANI. The optimized structures of the reference system were obtained by a density-functional tight-binding program (DFTB+) with basis sets from ref 41 and with a periodic boundary condition. The modeled systems are relaxed until the absolute value of the total interatomic forces is reduced to less than 10^{-4} atomic unit. The optimized structure of the PANI and its band diagram is shown in Figure 8, where the bands playing a major role in charge transport are shown in red. According to this presentation, the orbitals of PANI are delocalized over the main chain, and the highest

occupied states lie at the reciprocal vector of $k = (\pi/a, 0, 0)$ labeled as the "M" point on the diagram. Next, we have repeated the same calculations for PANI-MC and PANI-SP. The flexibility of the main chain (PANI) and of the alkyl chain covalently connecting a grafted molecule to the PANI leads to representative metastable structures of the PANI-SP and PANI-MC, which band diagrams and density of states (DOS) are summarized in Figure 9. According to our calculations, both of the systems seem to be conducting because the highest occupied band looks energetically close to the lowest unoccupied one in the vicinity of the Fermi level. However, the occupied states having a flat band do not contribute to hole transport because of low probability for electron interband transition, that is, electronic orbitals of the highest occupied states are localized at the side chains when, in the case of unoccupied states, orbitals are concentrated along the main chains (see Figure 8) of the polymer. Hence, the conductivity of the system in both cases (PANI-SP and PANI-MC) is affected by interband transition between the states where PANI's orbitals are delocalized over the main chains (highlighted in red) and, as a consequence, is influenced by the energy bandgap between those states. Our calculation presented in Figure 9 shows the effect of bandgap narrowing between the PANI-SP system (before irradiation, $E_g = 0.440$ eV) of the PANI-MC structure ($E_g = 0.268$ eV, after irradiation). Based on simulation results, the PANI-MC configuration tends to be more conductive than PANI-SP, which qualitatively comes in agreement with experimental results. The calculated bandgap narrowing suggests also an increase in probability in the thermal generation of free charge carriers, which in addition to the increase in hole mobility can both be attributed to the increase in the conductance of the system.

◼ CONCLUSIONS

This work shows that the covalent grafting of spiropyran to PANI nanowires resulted in a photochromic system. The electrical conductance of these photochromic PANI nanowires can be reversibly modulated by light irradiation. Our results indicate that the increase in the conductance is due to an increase in hole

mobility associated with the presence of large molecular dipoles of merocyanine. Additionally, band calculations of these structures show band gap narrowing of the system after UV irradiation, which qualitatively supports the experimental observations. In summary, such control over polyaniline's electrical properties holds a promise for optoelectronic nanodevices.

■ AUTHOR INFORMATION

Corresponding Author

*E-mail: sy@cc.huji.ac.il.

■ ACKNOWLEDGMENT

■ REFERENCES

(1) Cho, J.; Shin, K. H.; Jang, J. *Thin Solid Films* **2010**, *518*, 5066.

(2) Yoo, S. J.; Cho, J.; Lim, J. W.; Park, S. H.; Jang, J.; Sung, Y. E. *Electrochem. Commun.* **2010**, *12*, 164.

(3) Freitag, M.; Martin, Y.; Misewich, J. A.; Martel, R.; Avouris, P. *Nano Lett.* **2003**, *3*, 1067.

(4) Avouris, P.; Freitag, M.; PerPANIeinos, V. *Nat. Photonics* **2008**, *2*, 341.

(5) Ahn, Y.; Dunning, J.; Park, J. *Nano Lett.* **2005**, *5*, 1367.

(6) Hayden, O.; Agarwal, R.; LiPANIer, C. M. *Nat. Mater.* **2006**, *5*, 352.

(7) (a) Einaga, Y.; Sato, O.; Iyoda, T; Fujishima, A.; Hashimoto, K. *J. Am. Chem. Soc.* **1999**, *121*, 3745. (b) Einaga, Y.; Yamamoto, T.; Sugai, T; Sato, O *Chem. Mater.* **2002**, *14*, 4846. (c) Einaga, Y.; Taguchi, M.; Li, G.; Akitsu, T.; Gu, Z. Z.; Sato, O. *Chem. Mater.* **2003**, *15*, 8.

(8) Taguchi, M.; Li, G.; Gu, Z. Z.; Sato, O.; Einaga, Y. *Chem. Mater.* **2003**, *15*, 4756.

(9) Yamamoto, T.; Umemura, Y.; Sato, O.; Einaga, Y. *Chem. Mater.* **2004**, *16*, 1195.

(10) Mikami, R.; Taguchi, K.; Yamada, K.; Suzuki, K.; Sato, O.; Einaga, Y. *Angew. Chem., Int. Ed.* **2004**, *43*, 6135.

(11) Taguchi, M.; Yamada, K.; Suzuki, K.; Sato, O.; Einaga, Y. *Chem. Mater.* **2005**, *17*, 4554.

(12) Sirringhaus, H.; Kawase, T.; Friend, R. H.; Shimoda, T.; Inbasekaran, M.; Wu, W.; Woo, E. P. *Science* **2000**, *290*, 2123.

(13) Zhou, X.; Zifer, T.; Wong, B. M.; Krafcik, K. L.; Leonard, F.; Vance, L. A. *Nano Lett.* **2009**, *9*, 1028.

(14) Guo, X.; Huang, L.; Brien, O. S.; Kim, P.; Nuckolls, C. *J. Am. Chem. Soc.* **2005**, *127*, 15045.

(15) Hecht, D. S.; Ramirez, J. A. R.; Briman, M.; Artukovic, E.; Chichak, K. S.; Stoddart, J. F.; Gruner, G. *Nano Lett.* **2006**, *6*, 2031.

(16) Chen, S. A.; Liao, C. S. *Makromol. Chem. Rapid Commun.* **1993**, *14*, 63.

(17) Matsui, T.; Nagata, T.; Ozaki, M.; Fuji, A.; Onoda, M.; Teraguchi, M.; Masuda, M.; Yoshino, T. *Synth. Met.* **2001**, *119*, 599.

(18) Izumi, A.; Nomura, R.; Masuda, T. *Macromolecules* **2001**, *35*, 4342.

(19) Chen, Y.; Harrison, W. A.; Imrie, C. T.; Ryder, K. S. *J. Mater. Chem.* **2001**, *12*, 579.

(20) Martin, C. R. *Science* **1994**, *266*, 1961.

(21) Chiang, J. C.; MacDiarmid, A. G. *Synth. Met.* **1986**, *13*, 193.

(22) Wang, X.; Li, Y. *J. Am. Chem. Soc.* **2002**, *124*, 2880.

(23) Morales, A. M.; LiPANIer, C. M. *Science* **1998**, *279*, 208.

(24) Vandewyer, P. H.; Smets, G. *J. Polym. Sci., Part A* **1970**, *8*, 2361.

(25) Berkovic, G.; Krongauz, V.; Weiss, V. *Chem. Rev.* **2000**, *100*, 1741.

(26) Guo, X.; Zhang, D.; Yu, G.; Wan, M.; Li, J.; Liu, Y.; Zhu, D. *Adv. Mater.* **2004**, *16*, 636.

(27) Ipe, B. I.; Mahima, S.; Thomas, K. G. *J. Am. Chem. Soc.* **2003**, *125*, 7174.

(28) Neoh, K. G.; Kang, E. T.; Tan, K. L. *J. Polym. Sci., Part B: Polym. Phys.* **1993**, *31*, 355.

(29) Khor, S. H.; Neoh, K. G.; Kang, E. T. *J. Appl. Polym. Sci.* **1990**, *40*, 2015.

(30) Neoh, K. G.; Kang, E. T.; Tan, K. L. *J. Phys. Chem.* **1991**, *95*, 10151.

(31) Kang, E. T.; Neoh, K. G.; Tan, K. L.; Uyama, Y.; Morikawa, N.; Ikada, Y. *Macromolecules* **1992**, *25*, 1959.

(32) Tang, J.; Jing, X.; Wang, B.; Wang, F. *Synth. Met.* **1988**, *24*, 231.

(33) Wang, Z. H.; Epstein, A. J.; Ray, A.; MacDiarmid, A. G. *Synth. Met.* **1991**, *41*, 749.

(34) Kang, E. T.; Neoh, K. G.; Tan, K. L. *Prog. Polym. Sci.* **1988**, *23*, 277.

(35) Hwang, G. W.; Wu, K. Y.; Hua, M. Y.; Lee, H. T.; Chen, S. A. *Synth. Met.* **1998**, *92*, 39.

(36) Zhao, B.; Neoh, K. G.; Kang, E. T. *Chem. Mater.* **2000**, *12*, 1800.

(37) Peor, N.; Sfez, R.; Yitzchaik, S. *J. Am. Chem. Soc.* **2008**, *130*, 4158.

(38) Goykhman, I.; Korbakov, N.; Bartic, C.; Borghs, G.; Spira, M. E.; Shappir, J.; Yitzchaik, S. *J. Am. Chem. Soc.* **2009**, *131*, 4788.

(39) Tao, H.; Lu, M.; Yao, J.; He, C.; Di Spigna, N. H.; Nackashi, P. D.; Franzon, D. P.; Tour, J. *Adv. Mater.* **2008**, *20*, 4541.

(40) Yitzchaik, S.; Cabrera, I.; Buchholtz, F.; Krongauz, V. *Macromolecules* **1990**, *23*, 707.

(41) (a) Rauls, E.; Gutierrez, R.; Elsner, J.; Frauenheim, T. *Solid State Commun.* **1999**, *111*, 459. (b) Koehler, C.; Hajnal, Z.; Deak, P.; Frauenheim, T.; Suhai, S. *Phys. Rev. B* **2001**, *64*, 085333.(c) http://www.dftb-plus.info/.